Complete integrable particle methods and the recurrence of initial states for a nonlinear shallow-water wave equation

Roberto Camassa
Department of Mathematics
University of North Carolina at Chapel Hill
Chapel Hill, NC 27599

Long Lee
Department of Mathematics
University of Wyoming
Laramie, WY 82071

May 27, 2008

Abstract

We propose an algorithm for an asymptotic model of shallow-water wave dynamics in a periodic domain. The algorithm is based on the Hamiltonian structure of the equation and corresponds to a completely integrable particle lattice. In particular, "periodic particles" are introduced in the algorithm for waves travelling through the domain. Each periodic particle in this method travels along a characteristic curve of the shallow-water wave model, determined by solving a system of nonlinear integro-differential equations. We introduce a fast summation algorithm to reduce the computational cost from $O(N^2)$ to $O(N)$, where N is the number of particles. With the aim of providing a test of the algorithms, we scale the shallow-water wave equation to make it asymptotically equivalent to the KdV equation in the form studied by Zabusky and Kruskal in their seminal 1965 paper, thereby also testing the equivalence of the two models derived under similar asymptotic approximations of shallow water wave dynamics. By using the fast summation algorithm and the asymptotic scaling analysis, we further test this equivalence by investigating the interaction of solitons and recurrence of initial states for the shallow-water wave equation in periodic domains. Finally, to illustrate the hyperbolic nature of the dynamics of the shallow-water wave model, we introduce a particle algorithm and its integral counterpart for the initial-boundary value problem with homogeneous boundary conditions on finite intervals.

1 Introduction

The nonlinear partial differential equation (PDE) of evolution

$$u_t + 2\kappa u_x - u_{xxt} + 3uu_x = 2u_x u_{xx} + uu_{xxx} \tag{1.1}$$

results from an asymptotic expansion of the Euler equations governing the motion of an inviscid fluid whose free surface can exhibit gravity driven wave motion [5, 13]. The small parameters used to carry out the expansion are the aspect ratio, whereby the depth of the fluid is assumed to be much smaller than the typical wavelength of the motion, and the amplitude ratio, or ratio

between a typical amplitude of wave motion and the average depth of the fluid. Thus, the equation is a member of the class of weakly nonlinear (due to the smallness assumption on the amplitude parameter) and weakly dispersive (due to the long wave assumption parameter) models for water wave propagation. However, at variance with its celebrated close relatives in this class, such as the Korteweg-de Vries (KdV) and Benjamin-Bona-Mahony (BBM) equations, these small parameters are assumed to be linked only by a relative ordering, rather than a power law relation. This allows to retain terms on the right hand side that would be of higher order with respect to both the KdV and BBM expansions, and, in principle, consider dynamical regimes in which nonlinearity is somewhat dominant with respect to wave dispersion.

The above nonlinear equation possesses the remarkable property of complete integrability, as evidenced by its Lax-pair representation. Moreover, this property is complemented by the existence of a class of weak solutions that can serve as a natural projection of the general solution of (1.1) to an approximating (but still completely integrable) finite dimensional dynamical system [4, 6, 7]. This system of ordinary differential equations (ODEs) can be viewed as describing particle interacting through a long range potential (here position and momentum dependent), which expresses the fact that such particles are advected by the velocity u of the shallow water wave equation (1.1). The velocity is in turn determined by the particle positions and momenta. Previously such a particle system has been used to develop particle algorithms for solving the evolution equation (1.1) on the real line, and the "quarter-plane problem" with zero boundary condition at the origin [7]. Recently this particle algorithm has been extended to periodical domains, where "periodic particles" are introduced by summing all periods of the kernel in the system of integrable equations [8]. The present investigation focuses on developing the fast summation algorithm for this periodic case, and on using the particle method to study interaction of solitions and recurrences of initial states of the shallow water equation in periodic domains. The fast summation algorithm introduced in this paper reduces the computational cost from $O(N^2)$ to $O(N)$, where N is the number of particles. This algorithm is in particular suitable for studying cases, such as the recurrence behavior, that require extensive computations and large numbers of particles.

In the following sections, we briefly review the particle algorithm and its finite dimensional integrable system, followed by the introduction of the periodical particle method and a detailed discussion of the fast summation algorithm. We then proceed with several examples that illustrate the performance of the algorithm as well as present previously unexplored ranges of parameters and boundary conditions.

With an eye at comparing the asymptotic validity of the shallow-water wave equation (1.1) with respect to its classical counterparts such as the KdV equation, in Section 6 we scale (1.1) so that at leading order it is equivalent to the KdV equation discussed in [14]. Using the particle method and its fast summation algorithm, we observe interaction of "solitons" and the recurrence of initial states for the nonlinear shallow-water wave equation in a periodic domain. Such behaviors are similar to those reported in the paper of Zabusky and Kruskal [14].

In addition to periodic domains, and similar to the quater-plane problem discussed in [7], the homogeneous two-point boundary value problem for the nonlinear equation (1.1) can be represented by a particle system in terms of integral equations, so long as the Green's function of the operator $1 - \partial_x^2$ is uniquely determined according to the boundary conditions. Thus, we demonstrate how the particle method for the integration of the PDE (1.1) can be built so that each particle carries along the information from the boundary value problem. The fast summation algorithm for this particle method is also discussed, and numerical computations are carried out to show explicitly the effect of the particle "pile up" near the downstream interval boundary signaling the formation of a discontinuity for the PDE solution.

2 The integrable formulation and particle method

In this section we review briefly the particle algorithm developed in [4, 6, 7]. By introducing the characteristics $x = q(\xi, t)$,

$$\frac{dq}{dt} = u(q(\xi,t),t)\,, \qquad q(\xi,0) = \xi\,, \tag{2.1}$$

a solution of equation (1.1) in the infinite domain follows formally from the Hamiltonian system

$$\begin{aligned} q_t(\xi,t) &= \frac{1}{2}\int_{-\infty}^{\infty} e^{-|q(\xi,t)-q(\eta,t)|}p(\eta,t)d\eta - \kappa, \\ p_t(\xi,t) &= \frac{1}{2}\int_{-\infty}^{\infty} \operatorname{sgn}(\xi-\eta)\, e^{-|q(\xi,t)-q(\eta,t)|}\, p(\xi,t)p(\eta,t)d\eta. \end{aligned} \tag{2.2}$$

Here the characteristics $q(\xi,t)$ play the role of positions conjugate to the momentum-like variables $p(\xi,t)$ [4] in the Hamiltonian

$$H = \frac{1}{4}\int_{-\infty}^{\infty}\int_{-\infty}^{\infty}\Big(e^{-|q(\xi,t)-q(\eta,t)|}\,p(\eta,t)\,p(\xi,t) - \kappa\big(p(\xi,t)+p(\eta,t)\big)\Big)d\eta\,d\xi\,, \tag{2.3}$$

which yields system (2.2) by the (standard) Poisson structure

$$q_t = \frac{\delta H}{\delta p}\,, \qquad p_t = -\frac{\delta H}{\delta q}\,,$$

where $\delta/\delta q$, $\delta/\delta p$ denote functional derivatives with respect to the functions $q(\xi,t)$ and $p(\xi,t)$, respectively, at fixed time t. The choice of initial condition for the position variable, dictated by the characteristics condition, implies $q_\xi(\xi,0) = 1$, so that the constraint

$$q_\xi(\xi,t) = \frac{p(\xi,0)}{p(\xi,t)} \tag{2.4}$$

is maintained at all times of existence of the solution $(q(\xi,t), p(\xi,t))$. Thus, the momentum variable $p(\xi,t)$ could be eliminated from the system to obtain an evolution equation containing only the dependent variable $q(\xi,t)$ and its first derivative with respect to the initial label ξ. Vanishing of this derivative generically corresponds to crossing of characteristics curves, with loss of uniqueness of solutions $\xi(x,\cdot)$ to the equation $x = q(\xi,\cdot)$. Constraint (2.4) then shows that if the initial condition $p(\xi,0)$ does not have zeros, then $q_\xi(\cdot,t)$ is bounded away from zero, thereby preventing characteristics from crossing, for as long as $|p(\cdot,t)| < \infty$ [4]. The relation of system (2.2) with the original form (1.1) of the shallow water wave equation results from the definition of the velocity $u(x,t)$ in terms of characteristics $q(\xi,t)$ and the conjugate momentum $p(\xi,t)$,

$$u(x,t) = -\kappa + \frac{1}{2}\int_{-\infty}^{\infty} e^{-|x-q(\eta,t)|}p(\eta,t)\,d\eta\,. \tag{2.5}$$

System (2.2) can be rewritten in a slightly different form [6, 7], and the numerical algorithm proposed in [4] approximates the integrals in this system by their Riemann sums, thereby yielding Hamiltonian systems for "particles" with coordinates

$$q_i(t) \equiv q(\xi_i,t)$$

and momenta

$$p_i(t) \equiv p(\xi_i,t),$$

where $\xi_i = \Xi + ih$ for some real Ξ, step-size $h > 0$ and $i = 1, \cdots, N$.

By replacing the Jacobian q_η in the system of integrals with the constraint (2.4), the discretized version of the system results in the finite dimensional system of ODEs of N particles,

$$\begin{aligned}
\dot{q_i} &= \frac{h}{2}\sum_{j=1}^{N} e^{-|q_i - q_j|} p_j - \frac{h}{2}\,\kappa \sum_{j=1}^{N} e^{-|q_i - q_j|}\, p_j^0/p_j, \\
\dot{p_i} &= \frac{h}{2}\, p_i \sum_{i\neq j=1}^{N} \operatorname{sgn}(q_i - q_j) e^{-|q_i - qj|}\, p_j - \frac{h}{2}\,\kappa\, p_i \sum_{i\neq j=1}^{N} \operatorname{sgn}(q_i - q_j) e^{-|q_i - q_j|}\, p_j^0/p_j,
\end{aligned} \tag{2.6}$$

where $p(\xi_j, 0) \equiv p_j^0$. System (2.6) constitutes our *particle method* for solving the shallow-water wave equation (1.1); it can be shown to provide a convergent numerical algorithm to solutions of (1.1)under appropriate assumptions on the initial data [6, 7, 12].

3 The particle method in periodic domains

The particle method is extended to periodic domains in [8] by observing that periodic solutions $u(x,t)$ can be achieved by considering a periodic extension of the exponential kernel in (2.5) by superposition of period shifted exponentials (see also [1, 2])

$$\phi_L(x,q) = \sum_{k=-\infty}^{\infty} e^{-|x-(q+kL)|}, \tag{3.1}$$

where L is the period. We will refer to equation (3.1) as *the periodic kernel*. Equation (3.1) implies that one can always impose $0 \le |x-q| \le L$. We can express (3.1) in a more compact form by splitting the doubly infinite sum into its negative and positive index n range and looking at the two possible cases (1) $0 \le x - q \le L$ and (2) $-L \le x - q \le 0$. For case (1), we have

$$\begin{aligned}
\phi_L(x,q) =& \sum_{k=-\infty}^{0} e^{-(x-q)+kL} + \sum_{k=1}^{\infty} e^{(x-q)-kL} \\
=& \frac{e^{-(x-q)}}{1-e^{-L}} + \frac{e^{x-q}e^{-L}}{1-e^{-L}} \\
=& \frac{\cosh(x-q-L/2)}{\sinh(L/2)}.
\end{aligned} \tag{3.2}$$

Similarly, for case (2), the periodic kernel is

$$\phi_L(x,q) = \frac{\cosh(x-q+L/2)}{\sinh(L/2)}. \tag{3.3}$$

Combining (3.2) and (3.3), we have

$$\phi_L(x,q) = \frac{\cosh\big(|(x-q)_{\operatorname{mod} L}| - L/2\big)}{\sinh(L/2)}, \tag{3.4}$$

where $(x-q)_{\operatorname{mod} L}$ is modulo of $x-q$ and L, e.g., $(-8)_{\operatorname{mod} L} = 2$, if $L = 5$.

If we replace the kernel in the first equation of (2.2) by the periodic kernel (3.4) and integrate it over one period, we obtain an evolution equation for q

$$q_t(\xi,t) = \frac{1}{2}\int_{-L/2}^{L/2} \phi_L(q(\xi,t),q(\eta,t))\, p(\eta,t)\, d\eta - \kappa. \tag{3.5}$$

Taking the time derivative for the auxiliary function $p(\xi,t)$, as defined in [4] (equation (2.12) in that reference), and using (3.5), yields the evolution equation for p

$$p_t(\xi,t) = -\frac{1}{2}\, p(\xi,t) \int_{-L/2}^{L/2} \psi_L(q(\xi,t),q(\eta,t)) p(\eta,t)\, d\eta, \tag{3.6}$$

where

$$\psi_L(x,q) = \frac{\sinh\big(|(x-q)_{\mathrm{mod}\, L}| - L/2\big)}{\sinh(L/2)}. \tag{3.7}$$

Evaluating the integrals in (3.5) and (3.6) by the trapezoidal rule results in the finite dimensional system of ODEs of N particles in a periodic domain

$$\begin{aligned} \dot{q_i} &= \frac{h}{2}\sum_{j=1}^{N} \phi_L(q_i,q_j)p_j - \kappa \\ \dot{p_i} &= -\frac{h}{2}\, p_i \sum_{i\neq j=1}^{N} \psi_L(q_i,q_j)p_j. \end{aligned} \tag{3.8}$$

It is worth pointing out that since it is not necessary to resolve the numerical issue of a truncation of an infinite domain, a modified expression similar to (2.6) is not needed for the periodic case. The velocity $u_N(x,t)$ in terms of characteristics $q_i(t)$ and the conjugate momentum $p_i(t)$ is given by

$$u_N(x,t) = \frac{h}{2}\sum_{j=1}^{N} \phi_L(x,q_j(t))p_j(t) - \kappa. \tag{3.9}$$

Equations (3.8) and (3.9) constitute the periodic particle algorithm. A similar algorithm but based on a different perspective has been proposed in [12].

4 Fast summation algorithm

The major computational cost for the particle method is evaluating the Riemann sum in the finite dimensional system. The total operation count is in the order of $O(N^2)$ for N particles, if no particular speed up of the algorithm is devised. A recursion formula based on the absence of particle collision is introduced in [7] to reduce the cost from $O(N^2)$ to $O(N)$. In this section, we modify the recursion algorithm in [7] to develop a fast summation algorithm for summing the periodic kernels in the finite dimensional system. Such fast summation algorithms make use of the no-collision principle to strip the absolute value in the argument of the exponential function, which in turn makes a recursion relation for evaluating the sums possible. It is worth pointing out that while the periodic kernel has the compact expression (3.4), it is not possible to take advantage of this formula to develop the fast summation algorithm in periodic domains. The reason is that the hyperbolic functions used in the compact formula cause overflow in computing the recursion functions, if the period L is too large. Formula (3.1) is preferred for the following derivation.

Since κ in the $\dot{q}$ equation of system (3.8) is just some arbitrary constant which could always be absorbed by a redefinition of q, without loss of generality we assume $\kappa = 0$ in our derivation. With an eye at developing the recursion relation, we split the summation of index k in (3.1) into three parts, $k = 0$, sum of $k < 0$, and sum of $k > 0$. i.e., the $\dot{q}$ equation of (3.8) can be written as

$$\begin{aligned}\dot{q}_i &= \frac{h}{2}\sum_{j=1}^{N}\sum_{k=-\infty}^{\infty} e^{-|q_i-(q_j+kL)|}p_j \\ &= \frac{h}{2}\sum_{j=1}^{N}\sum_{k=-\infty}^{-1} e^{-|q_i-(q_j+kL)|}p_j + \frac{h}{2}\sum_{j=1}^{N} e^{-|q_i-q_j|}p_j + \frac{h}{2}\sum_{j=1}^{N}\sum_{k=1}^{\infty} e^{-|q_i-(q_j+kL)|}p_j,\end{aligned} \tag{4.1}$$

where $0 \le |q_i - q_j| \le L$. The second summation term (the $k = 0$ case) in the above equation can be dealt with in exactly the same way as in [7], while recursion formulas for the other two double summation terms are handled as follows:

Case 1, $k < 0$:

$$\begin{aligned}&\sum_{j=1}^{N}\sum_{k=-\infty}^{-1} e^{-|q_i-(q_j+kL)|}p_j \\ =&\sum_{j=1}^{N}\sum_{k=-\infty}^{-1} e^{-(q_i-q_j)+kL}p_j \\ =&\sum_{j=1}^{N} e^{-(q_i-q_j)}p_j \sum_{m=1}^{\infty} e^{-mL} \\ =&\frac{e^{-L}}{1-e^{-L}}\sum_{j=1}^{N} e^{-(q_i-q_j)}p_j.\end{aligned} \tag{4.2}$$

This leads to a recursion relation for (4.2) by letting

$$g_i^- \equiv \left(\frac{e^{-L}}{1-e^{-L}}\right)\sum_{j=1}^{N} e^{-(q_i-q_j)}p_j, \text{ so that } \quad g_{i+1}^- = e^{-(q_{i+1}-q_i)}g_i^-.$$

Similarly,

Case 2, $k > 0$:

$$\sum_{j=1}^{N}\sum_{k=1}^{\infty} e^{-|q_i-(q_j+kL)|}p_j = \frac{e^{-L}}{1-e^{-L}}\sum_{j=1}^{N} e^{(q_i-q_j)}p_j, \tag{4.3}$$

and

$$g_i^+ \equiv \left(\frac{e^{-L}}{1-e^{-L}}\right)\sum_{j=1}^{N} e^{(q_i-q_j)}p_j, \text{ so that } \quad g_{i+1}^+ = e^{(q_{i+1}-q_i)}g_i^+.$$

Using the same notation and recursion relation as in [7] (equations (4.2) and (4.4)therein), i.e.,

$$f_i^l = \sum_{j=1}^{i-1} e^{-(q_i-q_j)}p_j\,, \quad \text{and} \quad f_i^r = \sum_{j=i+1}^{N} e^{-(q_j-q_i)}p_j\,, \tag{4.4}$$

where

$$f_{i+1}^{l} = e^{-(q_{i+1}-q_i)}\big(f_i^{l} + p_i\big), \quad \text{and} \quad f_{i+1}^{r} = e^{-(q_i-q_{i+1})} f_i^{r} - p_{i+1}, \tag{4.5}$$

we have

$$\begin{aligned} \dot{q}_i =& \frac{h}{2}\big(g_i^{-} + f_i^{l} + p_i + f_i^{r} + g_i^{+}\big), \\ \dot{p}_i =& \frac{h}{2}\big(g_i^{-} + f_i^{l} - f_i^{r} - g_i^{+}\big)p_i\,. \end{aligned} \tag{4.6}$$

Note that we have a negative g_i^{+} in the $\dot{p}_i$ equation, since $\operatorname{sgn}\big(q_i - (q_j + kL)\big) < 0$ for $k > 0$.

5 Numerical examples

The shallow water equation (1.1) admits periodic travelling wave solutions $u(x,t) = U(x - c\,t)$ expressed implicitly by the elliptic function $\Pi(\varphi, \alpha^2, k)$ [3]. A specific example can be provided by taking the mean mass of the wave to be such that the minima of u are located at $u = 0$, and the wave elevation is positive. In this case one finds the solution of the travelling wave equation

$$U' = \pm\sqrt{\frac{-U^3 + (c - 2\kappa)U^2 + C(A)\,U}{c - U}} \tag{5.1}$$

where the integration constant $C(A)$ is a function of the wave amplitude A. Integration of equation (5.1) implies that the traveling wave solution U can be found by the following implicit equation,

$$x = \frac{2}{\sqrt{a_1(a_2 - a_3)}}(a_1 - a_2)\Pi(\varphi, \alpha^2, k)\,. \tag{5.2}$$

Here φ is a function of the dependent variable U, while the constants a_i, $i = 1, 2, 3$ (ordered in magnitude as $a_3 < 0 < a_2 < a_1$), and the parameters k and α are defined in terms of the wave velocity c, and the amplitude A, respectively. These relations are:

$$\varphi = \arcsin\left(\sqrt{\frac{a_1}{a_2}\,\frac{a_2 - U}{a_1 - U}}\right),$$

$$\begin{aligned} A \equiv a_3 =& \frac{1}{2}\Big(c - 2\kappa - \sqrt{(c - 2\kappa)^2 + 4C}\Big) \\ a_2 =& \frac{1}{2}\Big(c - 2\kappa + \sqrt{(c - 2\kappa)^2 + 4C}\Big) \\ a_1 =& c\,, \end{aligned}$$

and

$$k = \sqrt{\frac{a_2}{a_1}\,\frac{a_1 - a_3}{a_2 - a_3}}, \quad \alpha = \sqrt{\frac{a_2}{a_1}}\,.$$

Thus, the wavelength L of this periodic solution is linked to the parameter κ, the wave speed c, and the wave amplitude A by the relation

$$L = \frac{4}{\sqrt{a_1(a_2 - a_3)}}(a_1 - a_2)\Pi(\phi, \alpha^2, k)\,.$$

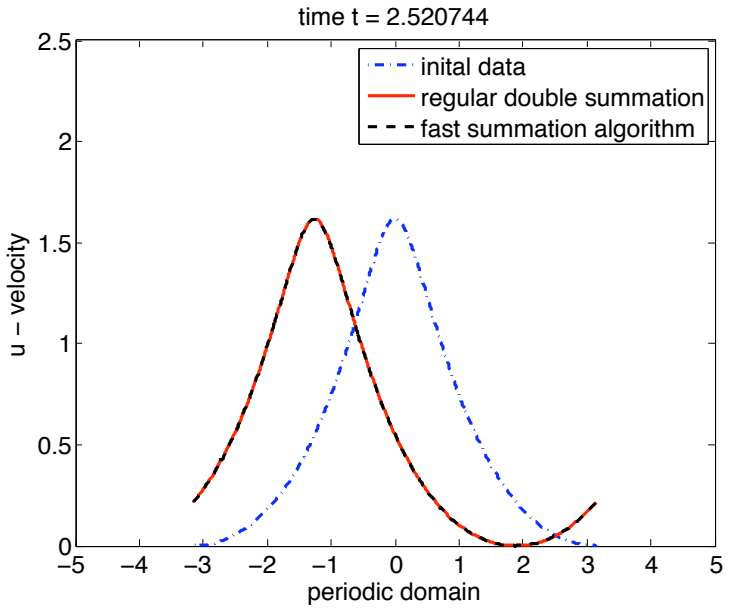

Figure 5.1: Comparison of the fast summation algorithm and the regular double summation method

While solution (5.2) may not have a direct physical interpretation, it can be used to test numerical schemes in the dispersive case, as illustrated next.

For the choice of parameters $c = 2$, $\kappa = 1/2$, and the integration constant $C = 1$, the wavelength (period) is $L \approx 6.3019$. The initial data (waveform) of the traveling wave solution, with data points $N = 512$, is the dot-dash line shown in Figure 5.1. Figure 5.1 also shows the snapshot of the traveling wave around time $t = 2.520744$. The solid line is the solution computed by the regular double summation method, while the dash line is the one computed by the fast summation algorithm. Not only both algorithms preserve the traveling waveform over this evolution time, but they are in fact visually indistinguishable. The time step used in this calculation is $\Delta t = 0.0158$. We compute this numerical example on an Apple Power G5 machine with a dual 2.7 GHz processor. The elapsed CPU time for the fast summation algorithm is less than 30 seconds, while the regular double summation method uses about 30 minute CPU time to compute the same result. Further results on convergence under grid refinement for the particle method in periodic domains are reported in [8].

6 Interaction of solitons and the recurrence of initial states

The KdV equation in the form

$$u_t + uu_x + \delta^2 u_{xxx} = 0\,, \tag{6.1}$$

in periodic domains for small δ^2, was brought to fame by the seminal paper of Zabusky and Kruskal [14] of 1965, in the course of investigating the intriguing recurrence phenomena exhibited by the FPU (from Fermi, Pasta and Ulam) lattice models of weakly nonlinear strings [11]. Zabusky and Kruskal used asymptotics to extract the KdV equation from the discrete lattice systems, and considered periodic smooth initial data analogous to those of FPU. After a near shock breaking

time, they observed the formation of solitary-wave pulses for which they coined the name "solitons," which moved uniformly at a rate linearly proportional to their amplitudes. The striking behavior reported for such solitons, since then understood to be the tell-tale sign and consequence of complete integrability in wave evolution equations, was that they passed through one another reappearing virtually unaffected in size or shape after their interaction. Remarkably, the recurrence phenomenon observed in FPU lattice was also reproduced for KdV, its asymptotic continuum model: the initial state would almost reappear after some time despite the soliton creation and interaction. The authors described the recurrence phenomenon as follows: "*In conclusion, we should emphasize that at T_R all the solitons arrive almost in the same phase and almost reconstruct the initial state through the nonlinear interaction.*" As shown in the context of its derivation as an asymptotic long wave model [5, 13], the nonlinear terms on the righ-hand-side of the shallow-water wave equation (1.1) are formally of higher order with respect to the KdV expansions. If we scale equation (1.1) to a dynamic regime in which wave dispersion balances nonlinearity, the dynamics of solutions should be comparable to those of the KdV equation (6.1). Thus, under such a scale and in periodic domains, the shallow-water wave equation should in principle support solutions that behave similarly to those of the KdV equation and exhibit phenomena similar to those described in Zabusky and Kruskal's paper [14], i.e. soliton formation with interactions, and the recurrence of smooth initial states.

Consider the initial value problem (IVP)

$$\begin{aligned} &u_t + uu_x + \delta^2 u_{xxx} = 0, \\ &u(x,0) = \cos \pi x, \\ &u(0) = u(2). \end{aligned} \tag{6.2}$$

Let $x' = x - ct$, $t' = t$, and $u' = \alpha u$. The above IVP can be rewritten as

$$\begin{aligned} &u'_{t'} - cu'_{x'} + \alpha u' u'_{x'} + \delta^2 u'_{x'x'x'} = 0, \\ &u'(x',0) = \frac{1}{\alpha} \cos \pi x', \\ &u'(0) = u'(2). \end{aligned} \tag{6.3}$$

For simplicity, we drop $'$ hereafter. Asumming that $\alpha^2 \ll \delta \ll \alpha \ll 1$, at the leading order, equations (6.3) become

$$\begin{aligned} &u_t - cu_x = O(\alpha,\, \delta^2), \\ &u(x,0) = \frac{1}{\alpha} \cos(\pi x), \\ &u(0) = u(2), \end{aligned} \tag{6.4}$$

which implies $u_{txx} = cu_{xxx} + O(\alpha, \delta^2)$. If we "blend" asymptotically equivalent terms by the relation

$$u_{xxx} = \mu u_{xxx} + (1-\mu) u_{xxx}, \tag{6.5}$$

we can write

$$u_{xxx} = \mu u_{xxx} + \left(\frac{1-\mu}{c}\right) u_{xxt} + O(\alpha, \delta^2). \tag{6.6}$$

Substituting equation (6.6) into equations (6.3), we obtain

$$\begin{aligned} &u_t - cu_x + \alpha u u_x + \mu\delta^2 u_{xxx} + \left(\frac{1-\mu}{c}\right)\delta^2 u_{xxt} = O(\alpha\delta^2, \delta^4), \\ &u(x,0) = \frac{1}{\alpha} \cos(\pi x), \\ &u(0) = u(2). \end{aligned} \tag{6.7}$$

Choosing $c = -1$ and $\mu = 0$, equations (6.7) become the initial value problem for the BBM system

$$\begin{aligned} &u_t + u_x + \alpha u u_x - \delta^2 u_{xxt} = O(\alpha\delta^2, \delta^4), \\ &u(x,0) = \frac{1}{\alpha}\cos(\pi x), \\ &u(0) = u(2). \end{aligned} \tag{6.8}$$

If we let $x' = \gamma x$ and $t' = t$, at the leading order we can write equations (6.8) as

$$\begin{aligned} &u_t + \gamma u_x + \alpha\gamma u u_x - \delta^2\gamma^2 u_{xxt} = O(\alpha\delta^2, \delta^4), \\ &u(x,0) = \frac{1}{\alpha}\cos(\pi x/\gamma), \\ &u(0) = u(2\gamma). \end{aligned} \tag{6.9}$$

Comparison of equations (1.1) with equation (6.9) yields the choice of parameters $\delta^2\gamma^2 = 1$, $\alpha\gamma = 3$, and $\gamma = 2\kappa$. This leads to $\gamma = 1/\delta$, $\alpha = 3\delta$, and $\kappa = 1/(2\delta)$. Substituting these parameters into equations (6.9), we obtain

$$\begin{aligned} &u_t + 2\kappa u_x + 3 u u_x - u_{xxt} = O(3\delta^3), \\ &u(x,0) = \frac{1}{3\delta}\cos(\pi\delta x), \\ &u(0) = u(2/\delta). \end{aligned} \tag{6.10}$$

Relations (6.10) represent the shallow-water wave equation (1.1) in scaled wave dispersion regimes. Therefore, under this set of scales equation (1.1) is compatible with the KdV equation (6.2), and we should expect to observe similar phenomena between the solutions of the two equations. We remark that based on the scaling analysis, when the parameter δ is small, the required periodic domain for the recurrence study for the shallow-water wave equation is large. Hence a large number of particles (or, equivalently, grid points for Eulerian based schemes) may be necessary for obtaining fully resolved computations. An $O(N)$ method, such as the particle method developed in this paper, becomes important for exploring the long-time behavior of the recurrence study for this equation. We also remark that the particle method, in contrast with its more general finite difference counterparts at the same order, shows evidence of improved accuracy for the process of generation of pulses from smooth initial conditions [6, 7, 8], which may prove advantageous for simulations where the creation process plays a relevant role. Figure 6.1 (a) is a recreation of Figure 1 in the paper of Zabusky and Kruskal [14] for the KdV equation (6.2), produced by the unconditionally stable spectral method developed in [9]. The result shows the temporal development of solitons emanating from smooth initial data $u(x,0) = \cos\pi x$. The small parameter δ in this calculation is 0.022. At time $t = t_B = 1/\pi$, u tends to develop a discontinuity at $x = 1/2$, and at $t = 3.6t_B$, all of eight solitons appear at the same time in the window of the periodic domain. Figure 6.1(b) is the result from the shallow-water wave equation, whose initial condition, period, and the parameter κ are scaled based on our previous analysis so that the equation is compatible with its KdV counterpart. The figures show that the solutions of the two equations share similar qualitative behaviors under the scaling. However, when observing the two figures closely, we see that while the number of solitons (i.e., number of peaks) is the same, and the feature of linearly decaying waveforms at intermediate times is very similar, the solitons' amplitudes and phases are different. Notice that in the scaling analysis the time variable in the two equations is the same, yet same-feature waveforms develop at different times between the two equations. For instance,

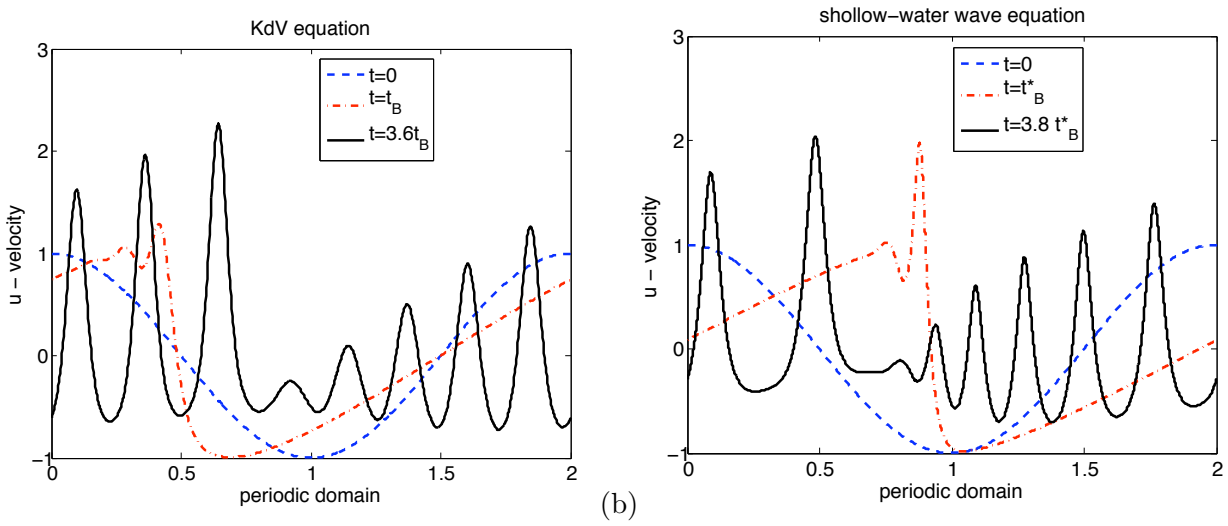

Figure 6.1: Comparison of the KdV and the shallow-water wave equation for the temporal development of solitons. (a) is a reproduction of Figure 1 in [14]. (b) is the counterpart from the shallow-water wave equation. The "breakdown" time for the KdV is $t_B = 1/\pi \approx 0.32$, and for the shallow -water wave equation is $t_B^* \approx 0.43$. The small parameter used for the KdV and the scaling analysis is $\delta = 0.022$, hence $\kappa = 1/(2\delta) \approx 22.7273$.

the KdV equation has the "breakdown" time $t_B = 1/\pi \approx 0.32$, whereas for the shallow-water wave equation this time is $t_B^* \approx 0.43$. Similarly, the time when all solitons can be discerned in the observation domain is $t \approx 1.46$ for the KdV equation, whereas this time is $t \approx 1.64$ for the shallow-water wave equation. Overall there is a small delay time shift Δt of about $0.1 \sim 0.2$ for the same phenomena to occur between the dynamics of the KdV and of the shallow-water wave equations in this example, with the shallow-water wave equation dynamics trailing behind. Our numerical experiments also show that such a delay depends on the initial condition and the magnitude of δ. We remark that in order to have a fair comparison between the two equations, the units in the plot of the shallow-water wave equation are scaled to be the same as for the KdV equation.

Next, we show an example of the recurrence of initial state for both the KdV and shallow-water wave equations in periodic domains. The initial condition is $u(x, 0) = 0.15\cos(\pi x)$ with the period $L = 2$ and $\delta = 0.022$. Figure 6.2 (a) shows the temporal development of the waveforms, and in particular a near recurrence of the initial state for the KdV equation. Figure 6.2 (b) shows the same features for the shallow-water wave equation evolution. We note that for this particular example and, in fact, for most of our experiments, the recurrence of initial states in the shallow-water wave equation dynamics is more closely achieved than for its KdV equation's counterpart. Figure 6.3 (a) and Figure 6.3 (b) show recurrences of the initial states (in different phases from the given initial conditions) for the KdV and shallow-water wave equation respectively. The figures clearly show that the recurrence for the shallow-water wave equation is closer to the initial data than in the case of the KdV equation: while this can be quantified in sup-norm, it can also be measured by more qualitative indicators such as the number of inflection points in the profile of the solution at recurrence. Consistently with the findings of Zabusky and Kruskal, our numerical experiments show that before a recurrence takes place, the solitons will go through three stages: (i) solitons appear at the same time in the domain, (ii) interaction of solitons, and (iii) all solitons appear again in the domain but ordered as the mirror image to stage (i) solitons. We illustrate this

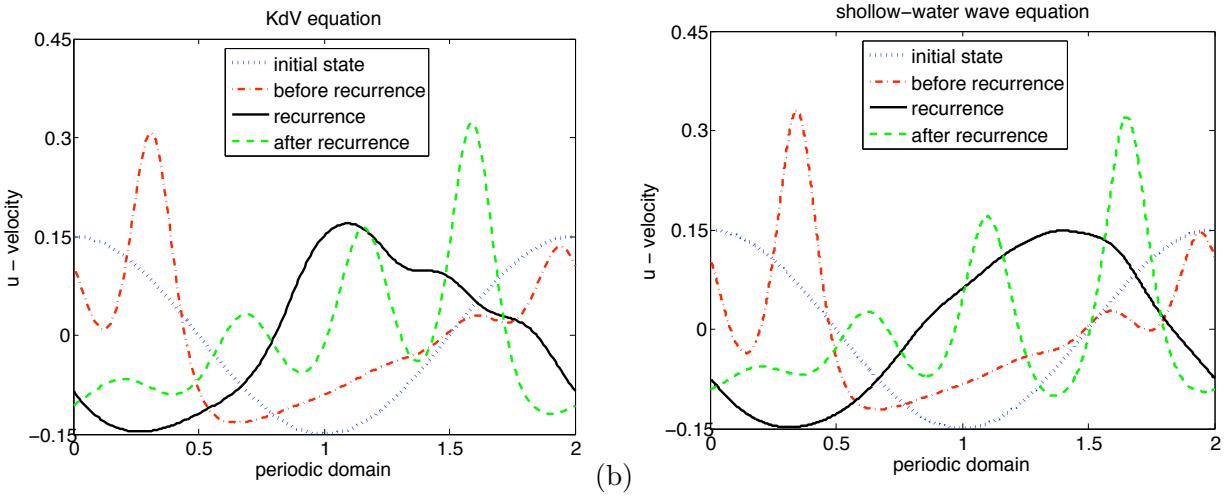

Figure 6.2: Comparison of the KdV and the shallow-water wave equation for a recurrence, and stages before and after the recurrence. The small parameter used for the KdV and the scaling analysis is $\delta = 0.022$, hence $\kappa = 1/(2\delta) \approx 22.7273$. The times for each stage are $t \approx 2.99$, 22.46, and 28.69 for the KdV equation, and $t \approx 4.02$, 26.05, and 31.98 for the shallow-water wave equation respectively.

reflectional symmetry in the next example, and show a case of "near super-recurrence," for which solitons arrive almost in the same phase and reconstruction of the initial state is nearly perfect. This case corresponds to the initial data $u(x,0) = 0.12/(3\delta)\cos(\delta\pi x)$ with the period $L = 2/\delta$ and the parameter $\kappa = 1/(2\delta)$, where $\delta = 0.018$. Figure 6.4 (a) shows that the solitons appear at the same time at $t = 8.38$, and Figure 6.4 (b) is the mirror image of (a), where $t = 26.08$.

In searching for the recurrence phenomenon for equation (1.1) exemplified above, the choice of parameters given by the matching with the KdV asymptotic scaling in [14] plays an important role. Recurrence of initial data at relatively short times appears to be dependent on the fine tuning of these parameters and can easily be pushed to several orders of magnitude longer times, especially as the number of solitary waves emerging from the initial data increases. Figure 6.5 illustrates this for the choice of smaller κ's (and larger δ's). The first time of quasi-recurrence shown in this figure appears at around time $t = 1900$. The somewhat delicate balance on parameters for the recurrence time deserves further investigation, which however is outside of the scope of this work and will be presented in a separate study.

After the mirror image is formed, Figure 6.6 shows a near super-recurrence at $t = 34.48$, with the waveform reconstructing the initial data.

While the particle method is an efficient and accurate algorithm for solving the shallow-water wave equation, the method is also advantageous for investigating the recurrence mechanism from the different perspective offered by the particle mechanical system. For the i^{th} "particle" in the particle system, q_i represents the particle coordinate while p_i is its conjugate momentum. Figure 6.7 plots $q - \xi$ vs ξ, where ξ is the initial coordinates of the particles. The slope of each plot is $q_\xi - 1$. When $q_\xi - 1 > 1$ particles compress to move and sharpen the waveform, while for $q_\xi - 1 < 1$ the situation reverses. Figure 6.7(a) suggests that particles compress in those regions where further interactions of the solitons are expected, whereas Figure 6.7(b) shows that particles are arranged to generate the reconstruction of the initial cosine wave.

Through particle interaction we see that when a recurrence occurs, both q and p shuffle to

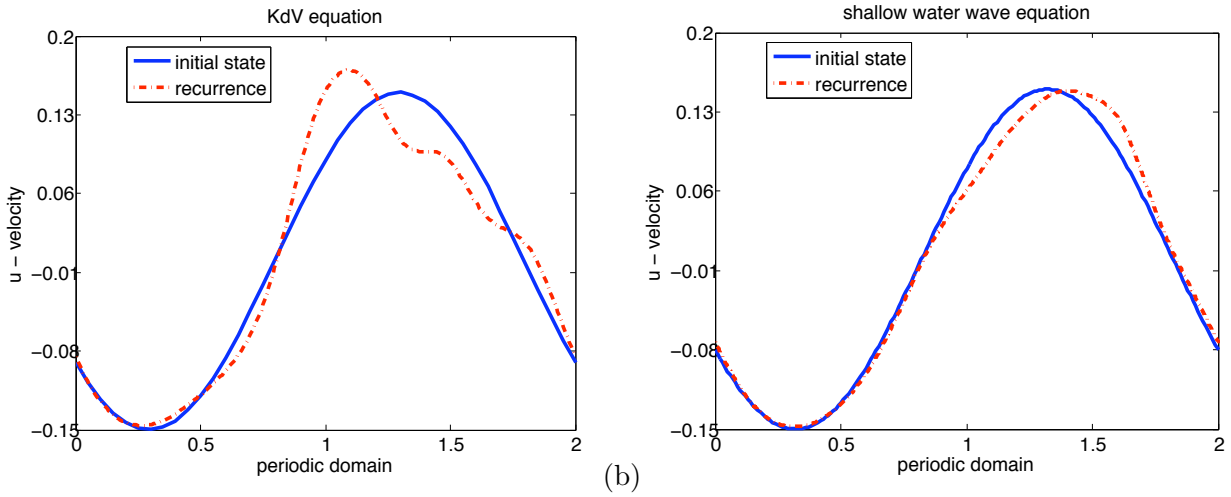

(a) (b)

Figure 6.3: Comparison of the recurrence of the initial states for the KdV and the shallow-water wave equation, exhibiting the closer match to the initial condition at a particular time. The time is $t \approx 22.46$ for the KdV equation, and $t \approx 26.05$ for the shallow-water wave equation respectively. The small parameter used for the KdV and the scaling analysis is $\delta = 0.022$, hence $\kappa = 1/(2\delta) \approx 22.7273$.

return to their initial states. Figure 6.8(a) is a plot for the momentum p vs the coordinate q; it shows that at $t = 34.48$, each particle possesses almost the same magnitude of momentum as the initial state. Figure 6.8(b) is the plot of $q - \xi$ vs ξ, which shows how particles return to equally distributed coordinates during the reconstruction. All the plots for the shallow-water wave equation are normalized by the parameter δ, except in Figure 6.5.

7 Particle and integral algorithms in finite domains

The particle method developed in [4, 6, 7] is extended to a quarter-plane problem with zero boundary conditions at the origin and at infinity of the positive real line. This problem maintains complete integrability as shown by the time invariance of the spectrum of an associated eigenvalue problem. In analogy to the quarter-plane problem, the homogeneous two-point boundary value problem for a finite interval can also be studied, with similar complete integrability properties (work in progress). In fact, the particle system can in turn be considered as a member of the family of Toda lattice flows, as the structure of the associated iso-spectral problem (Lax pair) [4] reveals, and it is of interest to consider this two point boundary value problem with an eye to future theoretical developments. Thus, in this last section, we develop a particle and an integral method for the shallow-water wave equation in finite domains with homogeneous boundary conditions.

Consider the following initial-boundary-value problem (IBVP) for the shallow-water wave equation (1.1),

$$\begin{aligned} &u_t + 2\kappa u_x - u_{xxt} + 3uu_x = 2u_x u_{xx} + uu_{xxx}, \\ &u(0,t) = u(L,t) = 0, \\ &u(0,x) = f(x), \quad 0 \le x \le L. \end{aligned} \tag{7.1}$$

For this IBVP, the Green's function associated with the operator $M = 1 - \partial_x^2$ has the form

$$G(x,y) = \frac{1}{2}\left(e^{-|x-y|}\right) + c_1(y)e^x + c_2(y)e^{-x}. \tag{7.2}$$

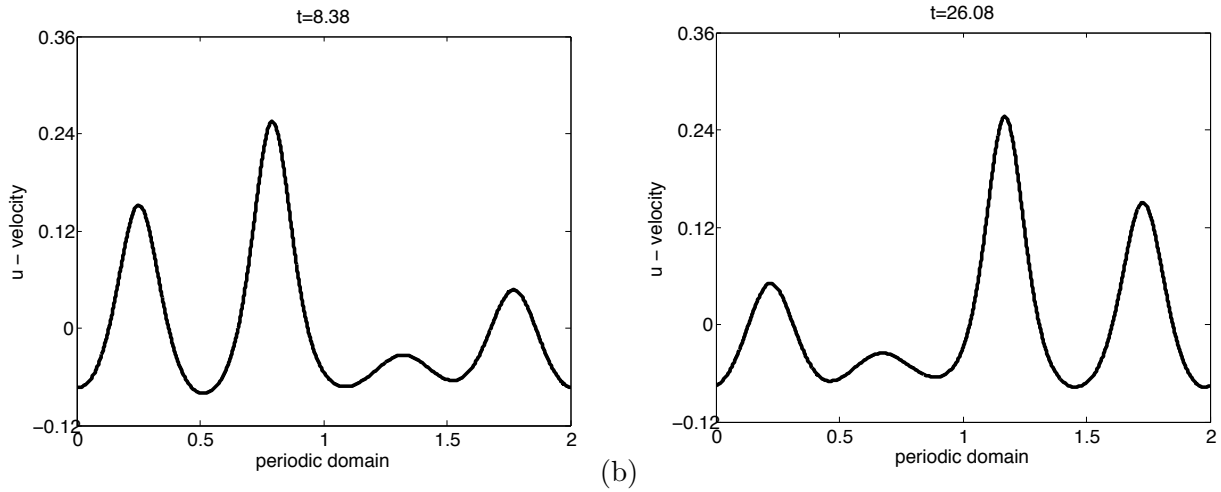

(a) (b)

Figure 6.4: Simulation corresponding to the small parameter for the scaling analysis $\delta = 0.018$ (hence $\kappa = 1/(2\delta) \approx 27.78$). Four solitons are formed. (a) First time all solitons appear fully formed in the domain. (b) Snapshot at time at which the position and the waveform of each soliton is the mirror image of the corresponding soliton in (a).

Applying the homogeneous boundary conditions, we obtain

$$G(x,y) = \frac{1}{2}\big(e^{-|x-y|} - e^{x-y}\big) + \frac{1}{2}\frac{\sinh(y-L)}{\sinh L}\big(e^{-x} - e^{x}\big). \tag{7.3}$$

The derivative of $G(x,y)$ with respect to x is

$$\Phi(x,y) = -\frac{1}{2}\big(\operatorname{sgn}(x-y)e^{-|x-y|} + e^{x-y}\big) - \frac{1}{2}\frac{\sinh(y-L)}{\sinh L}\big(e^{-x} + e^{x}\big). \tag{7.4}$$

Similarly, the derivative of $G(x,y)$ with respect to y is

$$G_y(x,y) = \frac{1}{2}\big(\operatorname{sgn}(x-y)e^{-|x-y|} + e^{x-y}\big) + \frac{1}{2}\frac{\cosh(y-L)}{\sinh L}\big(e^{-x} - e^{x}\big). \tag{7.5}$$

In analogy with equation (2.2), this Green's function and its derivative are the kernels of the integral equations of p and q for the IBVP. We present the evolution equation for q in a modified, but completely equivalent form to (2.2)

$$q_t(\xi,t) = \int_0^L G(q(\xi,t),q(\eta,t))\left(p(\eta,t) - \kappa\frac{\partial q}{\partial \eta}(\eta,t)\right)d\eta. \tag{7.6}$$

Once again, taking a time derivative to the function $p(\xi,t)$ and using equation (7.6), we obtain the evolution equation for p

$$p_t(\xi,t) = -p(\xi,t)\int_0^L \Phi(q(\xi,t),q(\eta,t))\left(p(\eta,t) - \kappa\frac{\partial q}{\partial \eta}(\eta,t)\right)d\eta, \tag{7.7}$$

For the purpose of evaluating the integral, the Jacobian q_η can be written as

$$\frac{\partial q}{\partial \eta}(\eta,t) = \frac{p(\eta,0)}{p(\eta,t)}, \tag{7.8}$$

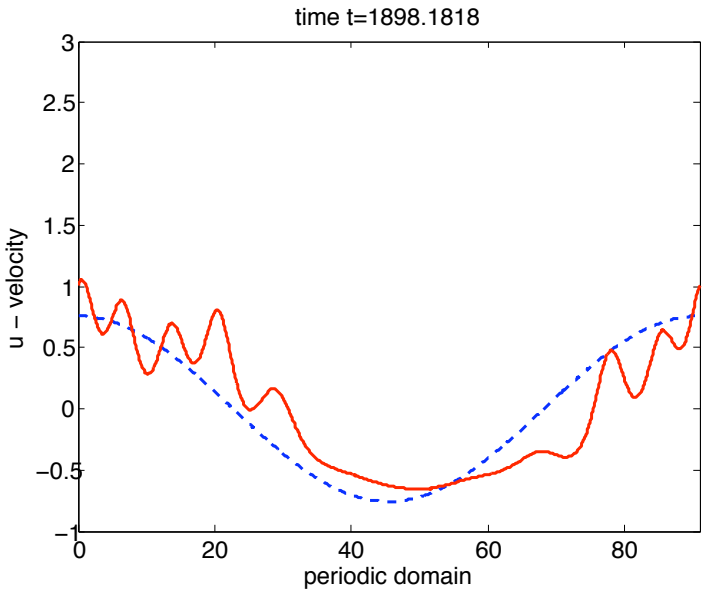

Figure 6.5: First quasi-recurrence for the shallow-water wave equation with the parameter choice $\kappa = 2$. The period is $L = 90.91$ and the amplitude of the initial data is 0.75. Notice the higher frequency oscillations with respect to the previous case in Figure 6.3(b).

where the equality was shown in [7]. If we apply the composite trapezoidal rule to the integral equations, we obtain a finite dimensional ODE system of N particles.

$$\begin{aligned}
\dot{q}_i =& \frac{h}{2} G(q_i, q_1)\left(p_1 - \kappa \frac{p_{0,1}}{p_1}\right) + h \sum_{j=2}^{N-1} G(q_i, q_j)\left(p_j - \kappa \frac{p_{0,j}}{p_j}\right) \\
&+ \frac{h}{2} G(q_i, q_N)\left(p_N - \kappa \frac{p_{0,N}}{p_N}\right) \\
\dot{p}_i =& -\frac{h}{2} p_i \Phi(q_i, q_1)\left(p_1 - \kappa \frac{p_{0,1}}{p_1}\right) - h p_i \sum_{j=2}^{N-1} \Phi(q_i, q_j)\left(p_j - \kappa \frac{p_{0,j}}{p_j}\right) \\
&- \frac{h}{2} p_i \Phi(q_i, q_N)\left(p_N - \kappa \frac{p_{0,N}}{p_N}\right),
\end{aligned} \tag{7.9}$$

where $p(\eta, 0) \equiv p_0$.

The derivative of the Green's function (7.5) can be substituted into the integro-differential equation derived in [7, 8] to obtain an integral algorithm for the IBVP,

$$u_t = -uu_x + \int_0^L G_y(x, y)\left(u^2 + \frac{u_y^2}{2} + 2\kappa u\right) dy. \tag{7.10}$$

Similar to the particle method, the above integral can be approximated by the composite trapezoidal method. We remark that the fast summation algorithms developed for evaluating the summation of the particle methods in infinite, semi-infinite, and periodic domains can be easily modified for

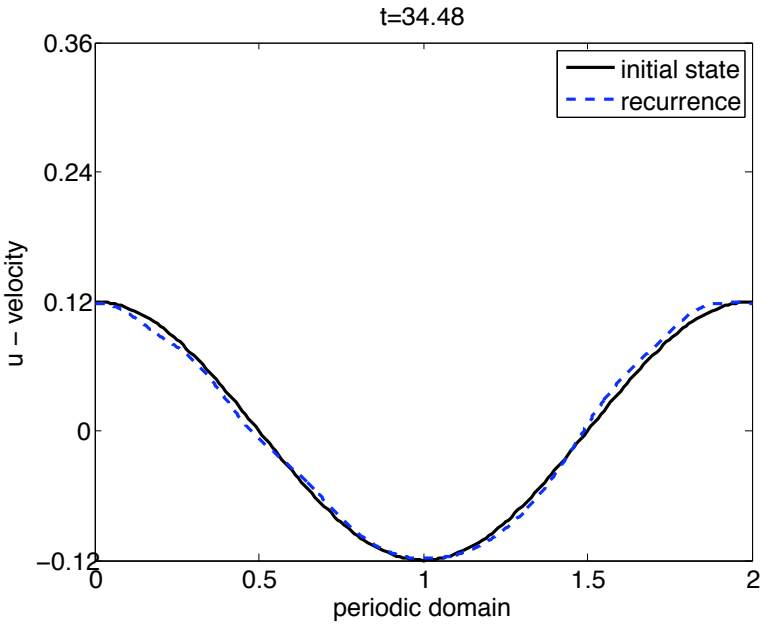

Figure 6.6: A continuation of Figure 6.4. It shows that a near super-recurrence occurres after the phenomena shown in Figure 6.4 are observed.

evaluating the summation in the trapezoidal method for the particle and the integral algorithms in this section.

Just as in the case of the Toda lattice [10], nonzero initial conditions and homogeneous boundary conditions may lead to shock formation. For the shallow water model, which is a unidirectional model, this can be understood (for $\kappa > 0$) by the fact that a zero boundary condition on the right-had-side will eventually stop waves traveling to the right, while the model does not allow for reflected waves to travel back into the domain away from that boundary. Hence we may expect a break-down to occur at the right boundary. For the case $\kappa = 0$ this physical interpretation no longer applies, which mathematically is reflected by the lack of a linearized form of the equation and hence of the dispersion relation. Thus, for this case there are no linear waves propagating from left to right and the break down can be expected to take longer to occur. This expected behavior of the continuum limit should be reflected by the particle approximating system, and we illustrate this with two examples next.

We consider the initial condition for the IBVP, $\sin x$ on the interval $L = [0, \pi]$. Figure 7.1 shows the evolution of u at time $t \approx 0.8639$, where (a) $\kappa = 1$ and (b) $\kappa = 0$. The black dot-dash line is from the integral method and the red solid line is from the particle method. They are visually identical. The number of particles used in the particle method is $N = 2000$, the same as the number of grid points used in the integral method. While u continues to evolve, particles accumulate near the boundary. If we blow up the waveforms near the right-hand-side boundary, we can observe some loss of smoothness. Figure 7.2 shows a blow-up of the solution near the boundary, where (a) $\kappa = 1$ and (b) $\kappa = 0$. After the solution develops irregularity near the boundary, the momenta p of the particles become very large and the particle method breaks down. The integral method can run to longer time after the formation of irregularity, but eventually breaks down as well. In this calculation we note that it takes a bit longer for the non-dispersive case $\kappa = 0$ to develop a

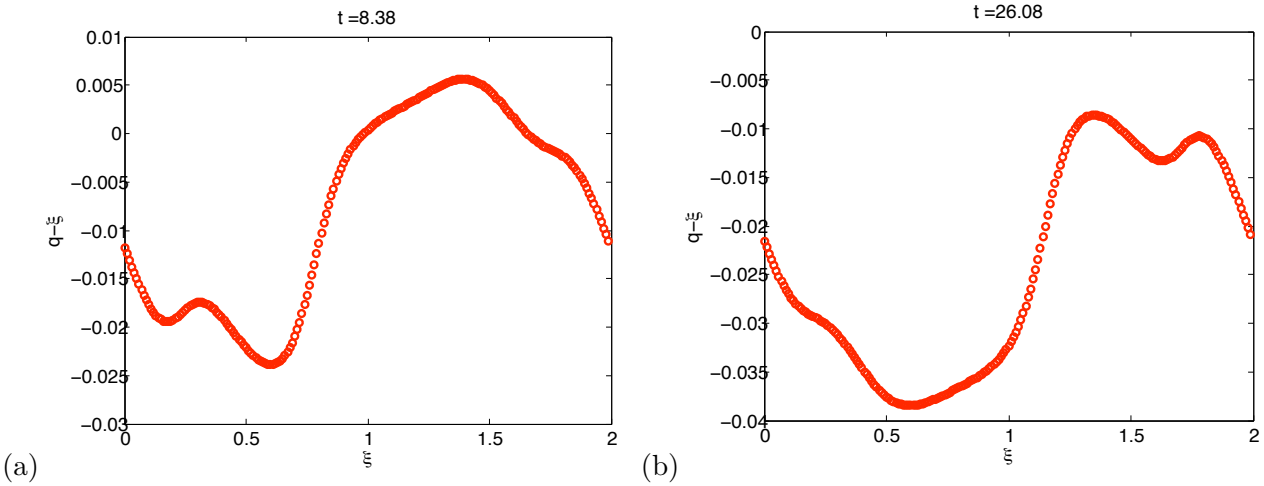

(a) (b)

Figure 6.7: Plots of $q - \xi$ vs ξ for Figure 6.4.

singularity at the boundary.

8 Discussion

We have extended the fast summation algorithms for the particle method developed in our previous work to the cases of periodic and finite interval homogeneous boundary conditions of the IBVP for the shallow water equation (1.1). With the speed-up afforded by the new algorithm, we have looked at the asymptotic closeness between evolutions from the same initial data in a periodic domain for the KdV and the shallow water wave equation, scaling variables so that both equations can be assumed to be formally equivalent asymptotic models of the same physical system. Our investigation shows that both models indeed share similar dynamical behavior for their solutions, and in particular the phenomenon of near recurrence of initial states, first discovered in weakly nonlinear FPU lattices, is exhibited in both dynamics. However, the recurrence for the shallow water case is more closely reminiscent of that observed in FPU lattices, and includes times of "super-recurrence," when the initial condition is almost perfectly recovered. Given the complete integrability of the underlying particle method, this phenomenon might be amenable to a detailed interpretation with finite dimensional dynamical system tools. With the aim at providing illustrations for future analytical investigations, we have also considered the two-point homogeneous boundary value problem, and in particular looked at the shock formation at the right boundary which can be expected from both physical and mathematical considerations due to the underlying hyperbolic structure of the shallow water model.

9 Acknowledgements

R. Camassa acknowledges support by NSF through grants DMS-0104329 and DMS-0509423. L. Lee thanks NSF for its support of the work through the grant DMS-0610149.

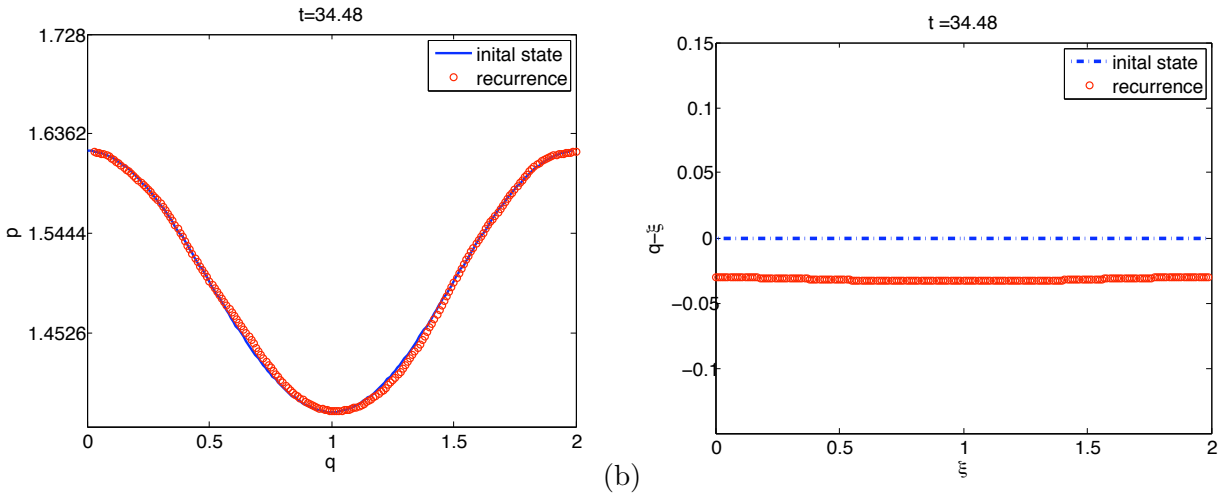

Figure 6.8: p and q at the initial state and at the time when the recurrence is observed (Figure 6.6): (a) particles' momenta p, and (b) particles' coordinates q.

References

[1] M.S. Alber, R. Camassa, D.D. Holm, J.E. Marsden. The geometry of peaked solitons and billiard solutions of a class of integrable PDEs. *Lett. Math. Phys.* , **32** (1994) 137-151.

[2] J.P. Boyd. Peakons and coshoidal waves: traveling wave solutions of the Camassa-Holm equation. *Appl. Math. Comput.*, **81** (1997) 173-187.

[3] P. F. Byrd and M. D. Friedman. *Handbook of Elliptic Integrals for Engineers and Physicists.* (1970), 2nd Edition, Springer.

[4] R. Camassa. Characteristics and the initial value problem of a completely integrable shallow water equation. *DCDS-B*, **3**, (2003) 115-139.

[5] R. Camassa, D. D. Holm, and J. M. Hyman. A new integrable shallow water equation. *Advan. Appl. Mech.*, **31**, (1994) 1-33.

[6] R. Camassa, J. Huang, and L. Lee. On a completely integrable numerical scheme for a nonlinear shallow-water wave equation. *J. Nonlin, Math. Phys.*, **12**, (2005) 146-162.

[7] R. Camassa, J. Huang, and L. Lee. Integral and and integrable algorithm for a nonlinear shallow-water wave equation. *J. Comp. Phys.*, **216**, (2006) 547-572.

[8] R. Camassa, and L. Lee. A completely integrable particle method for a nonlinear shallow-water wave equation in periodic domains. *DCDIS A*, **14**(S2), (2007) 1-5.

[9] T.F. Chan and T. Kerkhoven. Foruier methods with extended stability intervals for the Korteweg-de Vires equation. *SIAM Numer. Anal.*,**22**, (1985) 441-454.

[10] P. Deift and K. T-R McLaughlin. A continuum limit of the Toda lattice. *AMS Memoirs*, **624**, (1998) 1-216.

[11] E Fermi, J. R. Pasta, and S. Ulam. Los Alamos Scientific Laboratory No. LA-1940, May 1955 (unpublished).

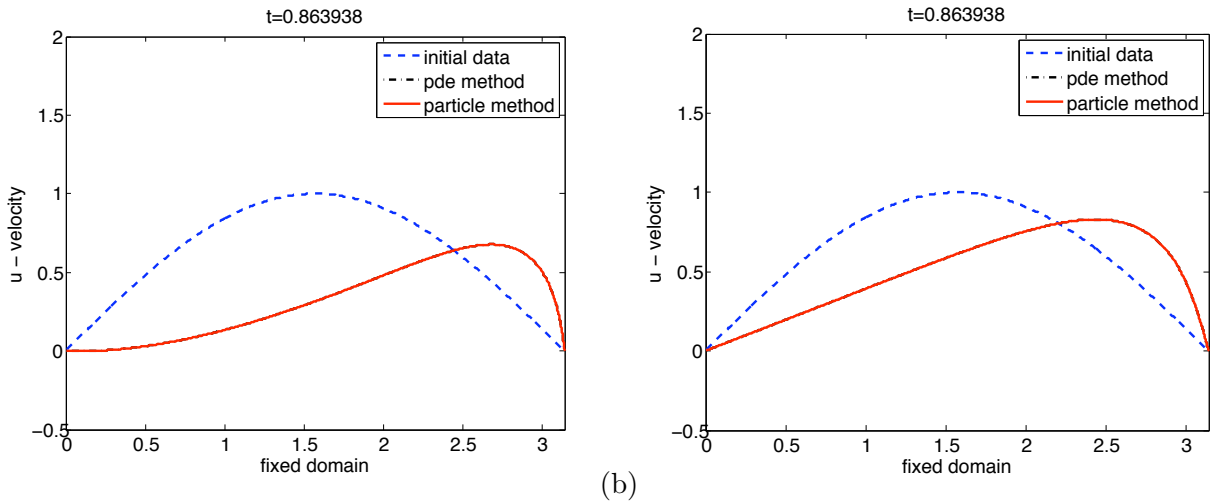

(a) (b)

Figure 7.1: The waveform before the break-down time, at $t \approx 0.863938$, from the particle and the integral algorithm, (a) $\kappa = 1$, (b) $\kappa = 0$.

[12] H. Holden and X Raynaud. A convergent numerical scheme for the Camassa-Holm equation based on multipeakons. *DCDS*, **14**, (2006) 505-528.

[13] R.S. Johnson Camassa-Holm, Korteweg-de Vries and related models for water waves. *JFM*, **455**, (2002) 63-82.

[14] N. J. Zabusky and M. D. Kruskal. Interaction of "solitons" in a collisionless plasma and the recurrence of initial states. *Phys. Rev. Lett.*, **15**, (1965) 240-243.

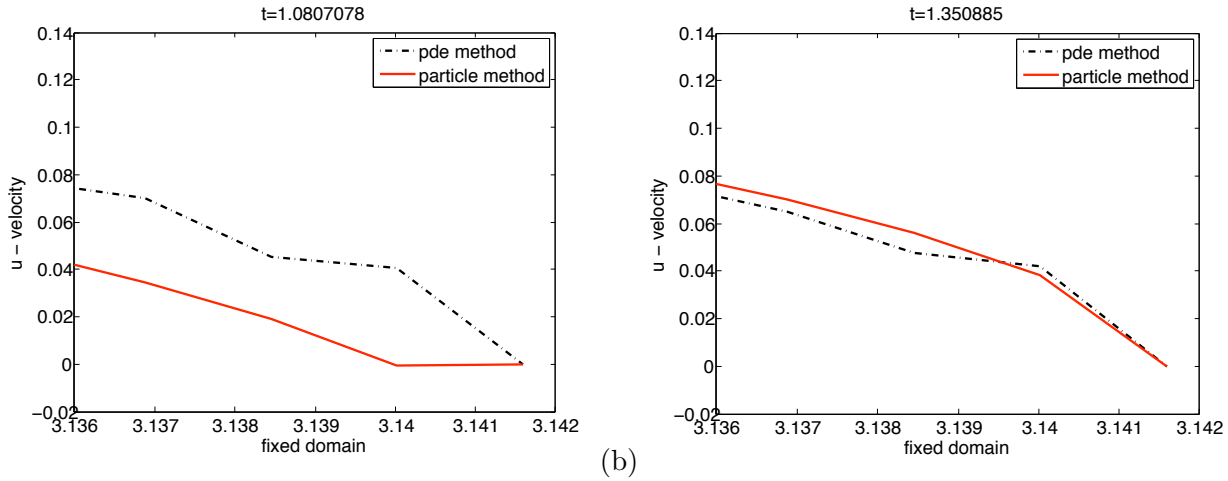

(a) (b)

Figure 7.2: The formation of irregularities near the boundary for both particle and integral methods, (a) $\kappa = 1$ at $t \approx 1.0807078$, (b) $\kappa = 0$ at $t \approx 1.350885$.